

A distributed piezo-polymer scour net for bridge scour hole topography monitoring

Kenneth J. Loh*, Caroline Tom, Joseph L. Benassini and Fabián A. Bombardelli

Department of Civil and Environmental Engineering, University of California, Davis, One Shields Avenue, 2001 Ghausi Hall, Davis, CA 95616, USA

(Received January 26, 2014, Revised May 16, 2014, Accepted June 4, 2014)

Abstract. Scour is one of the leading causes of overwater bridge failures worldwide. While monitoring systems have already been implemented or are still being developed, they suffer from limitations such as high costs, inaccuracies, and low reliability, among others. Also, most sensors only measure scour depth at one location and near the pier. Thus, the objective is to design a simple, low cost, scour hole topography monitoring system that could better characterize the entire depth, shape, and size of bridge scour holes. The design is based on burying a robust, waterproofed, piezoelectric sensor strip in the streambed. When scour erodes sediments to expose the sensor, flowing water excites it to cause the generation of time-varying voltage signals. An algorithm then takes the time-domain data and maps it to the frequency-domain for identifying the sensor's resonant frequency, which is used for calculating the exposed sensor length or scour depth. Here, three different sets of tests were conducted to validate this new technique. First, a single sensor was tested in ambient air, and its exposed length was varied. Upon verifying the sensing concept, a waterproofed prototype was buried in soil and tested in a tank filled with water. Sensor performance was characterized as soil was manually eroded away, which simulated various scour depths. The results confirmed that sensor resonant frequencies decreased with increasing scour depths. Finally, a network of 11 sensors was configured to form a distributed monitoring system in the lab. Their exposed lengths were adjusted to simulate scour hole formation and evolution. Results showed promise that the proposed sensing system could be scaled up and used for bridge scour topography monitoring.

Keywords: bridge scour; distributed sensing; piezoelectric sensor; scour monitoring; thin film; vibration monitoring

1. Introduction

Bridge scour, or the erosion of soil or earth material at bridge pier foundations by flowing water (Ayres 2004), is a leading cause of bridge failures worldwide (Deng and Cai 2010). Of nearly 500,000 overwater bridges, Gee (2008) has reported that ~21,000 of them have been classified as scour critical (i.e., the foundation has been deemed unstable due to scour) (Hunt 2009). In addition, 58% of the 1,502 documented bridge failures from 1966 to 2005 have been directly or indirectly caused by scour (Hunt 2009). If left undetected, structural failures such as the complete collapse of the 32 year-old Schoharie Creek Interstate Highway Bridge (Mohawk River, NY) in 1987 could

*Corresponding author, Associate Professor, E-mail: kjloh@ucdavis.edu

occur again. The potential catastrophic effects of bridge scour, the cost implications, and the threat to public safety have motivated the development and application of a wide variety of monitoring systems. The objective is to detect the onset of scour so that engineers can intervene and prevent structural failure (e.g., by installing scour countermeasures as suggested by Barkdoll *et al.* 2007).

Besides visual inspection, scour monitoring systems currently used in practice are classified as either fixed or portable instrumentations. Hunt (2009) and Lueker *et al.* (2010) have compiled detailed reports summarizing scour monitoring devices used. First, common fixed instrumentation devices include sonar, magnetic sliding collar, float-out devices, and tilt or vibration sensors, among others (Schall and Davies 1999). They are permanently installed on or near the bridge and can collect data at fixed time intervals. For example, sonar transducers mounted on a bridge pier would emit sound pulses towards the streambed and would measure the subsequent echo response times to determine scour depth (Deng and Cai 2010, Schall *et al.* 1997). While sonar can collect data over long time periods and store them in a data logger, provide manual downloads, or stream data to the Web, other devices such as float-out devices are single-use. When the scour hole propagates to a buried device, it floats to the water surface, and its built-in wireless transmitter sends a signal to a remote receiver indicating that scour has occurred (Hunt 2009). Second, portable scour instrumentation refers to systems that are temporarily used and installed, such as sounding rods. Their greatest limitation is the inability to provide continuous monitoring, particularly during times when the risk of bridge scour is greatest (e.g., during flooding, rapid river flow, or extreme weather). Although some bridges have already been instrumented with fixed bridge scour monitoring systems, their low reliability, high costs, maintenance, and vulnerability to damage have limited their effectiveness. In general, the inability to monitor scour, detect damage, and direct repair efforts lead to ineffective/inefficient infrastructure management, high maintenance costs, and unsafe structures.

These limitations have spurred research in developing novel scour monitoring systems, such as fiber Bragg grating (FBG) sensors (Lin *et al.* 2006, Zhou *et al.* 2011), wireless sensors (Liu *et al.* 2010), optical fiber vibrating rods (Zarafshan *et al.* 2012), piezoelectric transducers (Wang *et al.* 2012), and inductively coupled systems (Radchenko *et al.* 2013), among others. Some of these technologies have been subjected to extensive laboratory testing, whereas others have even been validated in the field. While each technological alternative offers unique advantages as compared to conventional scour monitoring solutions, these prototypes are still in their early stages of development. Most of these sensors also only measure scour depth at one location and near the bridge pier.

In this study, a simple, low cost, laboratory-scale scour monitoring system (termed Scour Net) is proposed for monitoring 3D scour hole topography and scour hole evolution over time. The objective is to design and validate the performance of a piezoelectric polymer sensor strip mounted as a cantilevered beam and buried in the streambed. Scour would erode sediments and expose the sensor strip. Flowing water would then excite the exposed portion of the sensor to cause it to oscillate. The dynamics of the oscillations depend on the length of the exposed sensor strip or scour depth. Since piezoelectric materials generate electrical charge in response to time-varying strains, the sensor is self-sensing and does not depend on an external power source for operations (Wang *et al.* 1988). However, unlike Wang *et al.* (2012) who have used a set of discrete piezoelectric films for determining scour depth at one location, this work employs a continuous film. The main advantage is that only one data acquisition channel is needed per sensor, as opposed to eight or more per measurement location (Wang *et al.* 2012). In order to resolve scour depth, a simple signal processing method has been implemented for calculating the sensor's

resonant frequency (which is related to the exposed length of the sensing strip). The procedure adopted is comparable to that by Zarafshan *et al.* (2012), except their algorithm has been designed for FBG sensors. Lastly, the proposed piezoelectric sensor can be instrumented in a densely distributed fashion to track changes in the shape, size, and depth of a scour hole. Here, the goal is to demonstrate proof-of-concept, and tests are conducted in idealized laboratory conditions to obtain preliminary results that will be used to guide future, more sophisticated studies.

This paper begins with a detailed description of the design and fabrication of each Scour Net piezoelectric strip. Second, the signal processing method for determining scour depth is outlined. Then, a series of experiments conducted in the laboratory are presented. In total, three sets of tests are discussed: (1) validation and calibration of a single sensor in ambient air; (2) proof-of-concept in a water tank; and (3) demonstration of scour hole topography monitoring. Finally, the paper concludes with a summary of major findings and future research directions.

2. Sensor design and background

The design of Scour Net was based on mounting a piezoelectric polymer sheet onto the surface of a thin poly-(dimethylsiloxane) (PDMS) elastomer strip. Each sensor could be buried in the streambed (e.g., at a location where scour was prone to occur or near a bridge pier) and perpendicular to the direction of water flow (Fig. 1). In the absence of scour, the sensor would remain buried and would not output a response. In the event of scour, fluid flow would excite and cause the exposed cantilevered sensor to vibrate. The piezoelectric strip would respond to these vibrations by generating a time-varying voltage signal. The voltage time history and the resonant frequencies of oscillation were used for determining the exposed sensor length, which was also the scour depth at that location. This section continues with a discussion of sensor fabrication, data acquisition, followed by signal processing.

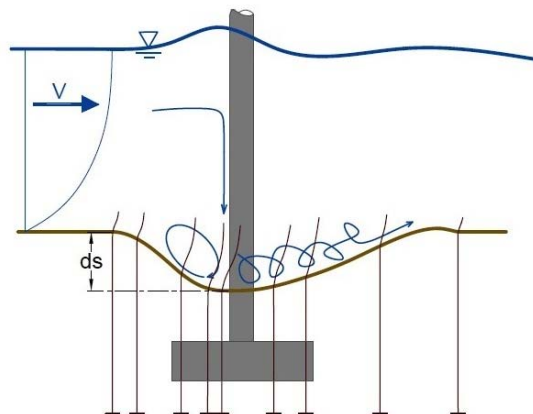


Fig. 1 The schematic illustrates the operating principle of the distributed Scour Net monitoring system. Buried cantilevered piezoelectric strips become exposed due to scour hole evolution

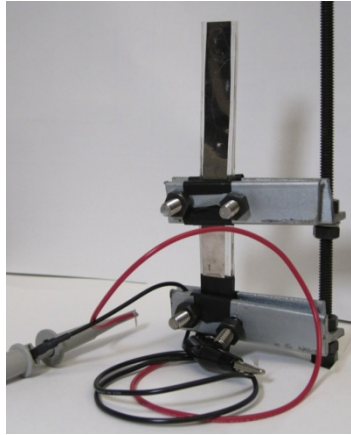


Fig. 2 A Scour Net sensor was configured to form a vertical cantilevered beam and was attached on a customized mount for experimental testing. The exposed length was adjusted by sliding the top security mount up or down (i.e., for simulating scour)

2.1 Scour net sensor fabrication

The design of the distributed scour depth sensor was based on affixing or embedding piezoelectric sensor strips in a PDMS elastomer substrate. PDMS was selected for its low cost, chemical inertness, water resistance, low coefficient of thermal expansion, and ease of manufacturing (Ryu *et al.* 2011). It was also a flexible elastomer that could be casted to different geometries, thicknesses, and sizes. First, manufacturing of the PDMS substrate was based on using the *Sylgard* 184 PDMS silicone elastomer kit from Dow Corning. The two components of the kit included the PDMS base (Part I) and the curing agent (Part II). Second, PDMS Parts I and II were measured and mixed together at a 10:1 (by weight) ratio. The mixture was then stirred vigorously by hand in a large Pyrex beaker for ~2 min, before it was poured into a rectangular ($18 \times 13 \times 4 \text{ cm}^3$) Pyrex glass container. Next, the PDMS mixture and container was cured in a vacuum oven operating at $80 \text{ }^\circ\text{C}$ for 4 to 5 h. Finally, the cured PDMS elastomer was cooled at room temperature and then cut to thin rectangular strips approximately 18 cm long, 2 cm wide, and 0.3 cm thick.

Sensor fabrication continued with mounting of a commercial poly (vinylidene fluoride) (PVDF)-based film onto the cut PDMS strip. In this study, metallized Piezo Film from Measurement Specialties (i.e., a PVDF-based piezoelectric polymer coated on both sides with silver ink and nickel-copper alloy electrodes) was employed as the sensing element. Pristine Piezo Films from the manufacturer were $20 \times 28 \text{ cm}^2$ and $110 \text{ }\mu\text{m}$ thick, and they were cut to smaller rectangular strips of $\sim 15 \times 1.5 \text{ cm}^2$ using a razor blade. Once cut, the electrodes were formed by soldering wires to copper tape and then by affixing them onto the metallized surfaces. Conductive silver paste was also painted over the metallized surface and copper tape for minimizing contact resistance. For sensor validation tests that were conducted in air, the Piezo Film was affixed onto the PDMS surface using 3M double-sided tape (Fig. 2). The use of double-sided tape was because of its convenience and the ease of removing/reusing the Piezo Films. Nevertheless, good strain transfer between the sensor and substrate was observed. On the other hand, tests conducted in wet environments required that the piezoelectric sensor be waterproofed; thus, the Piezo Film ($\sim 30 \times 1.5$

cm²) was embedded in the PDMS substrate during casting. The embedded sensor was then affixed onto a 1.5 mm-thick poly-(vinyl chloride) (PVC) plate for additional support and rigidity.

2.2 Data acquisition

A four-channel Agilent MSO8104A oscilloscope was employed as the data acquisition (DAQ) system for interrogating Scour Net. An oscilloscope was used because it provided the greatest flexibility (i.e., voltage range, sampling rates, and high resolution), which was necessary before a permanent DAQ solution was devised. However, since it is unrealistic to query the sensors using MHz or GHz sampling rates, the DAQ's sampling rate was manually set to 50 kHz (the minimum allowable) and triggered to record 10 s-long voltage time histories. Depending on the test, either one, some, or all four channels were used to query sensors simultaneously.

2.3 Signal processing

A signal processing algorithm was implemented in *MATLAB* for processing Scour Net measurements and for calculating scour depth. As mentioned earlier, if a portion of the piezoelectric sensing strip were to become exposed due to scour, the surrounding flowing water (or air in some preliminary tests) would excite and cause it to vibrate. These vibrations (i.e., dynamic strains) caused the Piezo Film and Scour Net sensor to generate a corresponding time-varying voltage signal.

In fact, the dynamics of the exposed sensor strip was captured by the voltage responses. Thus, a Fast Fourier Transform (FFT) was performed to map time-domain voltage response data to the frequency-domain. The first fundamental vibration mode was identified using the first major peak of the power spectral density (PSD) function. It should be mentioned that, one could narrow the search of the first resonance peak to a narrow band of frequencies (typically between 2 to 100 Hz) since the geometry of the Scour Net was known *a priori*. Also, by assuming that the cantilevered Scour Net was a single degree-of-freedom (SDOF) system, its resonant frequency (f) or natural frequency (ω_n) could also be expressed in terms of its structural stiffness (k) and mass (m) as shown in Eq. (1)

$$f = \frac{\omega_n}{2\pi} = \frac{1}{2\pi} \sqrt{\frac{k}{m}} \quad (1)$$

Damping was not considered in this proof-of-concept study, but it should be mentioned that its value could be significant when the sensors were to be deployed in wet or riverine environments. The density (ρ) of the cantilevered sensor could also be determined by measuring its mass and spatial dimensions (exposed length L , thickness t , and width w using a digital caliper) in the laboratory.

$$\rho = \frac{m}{Lwt} \quad (2)$$

It should be mentioned that L is the parameter of interest. The average density, after five specimens were measured and weighed, was found to be 988 kg-m⁻³.

Keeping with the assumption that the Scour Net was a SDOF dynamic system, the stiffness of a cantilevered structure could be calculated using Eq. (3)

$$k = \frac{3EI}{L^3} \quad (3)$$

where E is the Young's modulus of the entire Piezo Film and PDMS composite system, and I is the second moment-of-inertia for the sensor's rectangular cross-section (Eq. (4)).

$$I = \frac{wt^3}{12} \quad (4)$$

Other studies already investigated the Young's modulus of *Sylgard 184* PDMS. For example, Schneider *et al.* (2008) reported that E was 1.82 MPa. For this study, the PDMS-based sensor was not load tested to determine E , since the integrated Piezo Film made testing challenging. Instead, a set of piezoelectric sensor test results (as will be discussed later) were used to calibrate and estimate E . One reason this approach was employed was that E for the composite sensor with PVDF, tape, and PDMS could not be determined easily and accurately using analytical calculations. Lastly, since the goal was to estimate Scour Net exposed length, Eqs. (1)-(4) were combined to express L in terms of known physical parameters and the measured resonant frequency of the sensor

$$L = \left[\frac{Et^2}{4(2\pi f)^2 \rho} \right]^{1/4} \quad (5)$$

Eq. (5) was used to calculate scour depth at each sensor location. Eq. (5) does not depend on the width of the sensor, as long as it remained constant for the entire length.

3. Piezoelectric sensor validation

Once the Scour Net piezoelectric sensors were fabricated, two sets of tests were performed to validate scour depth monitoring. The first test involved using the piezoelectric sensor as a cantilevered structure in ambient air. The length of the cantilevered segment was varied, and free vibration results were used for back-calculating its lengths. Then, a second test was conducted in a more realistic operating environment where the Scour Net was submerged underwater and buried in sand.

3.1 Sensor performance characterization and calibration

The objective of the first set of laboratory tests was to characterize the performance of the Scour Net sensor in a controlled dry environment. A customized mount was machined so that Scour Net sensors fitted on top of a Newport optics table to form a vertical cantilevered beam (Fig. 2). The sensor was also connected to an Agilent MSO8104A DAQ as mentioned earlier. Then, free vibration of the cantilevered sensor was induced by manually introducing an initial displacement. Here, one or multiple free vibration responses were induced during each 10 s-long test. This test began with an exposed length of 1 cm, which was then increased to 9 cm (in 1 cm increments). As an added precaution, each exact exposed length was also measured using a digital caliper (0.01 mm resolution). Two to four sets of data were collected for each exposed length case.

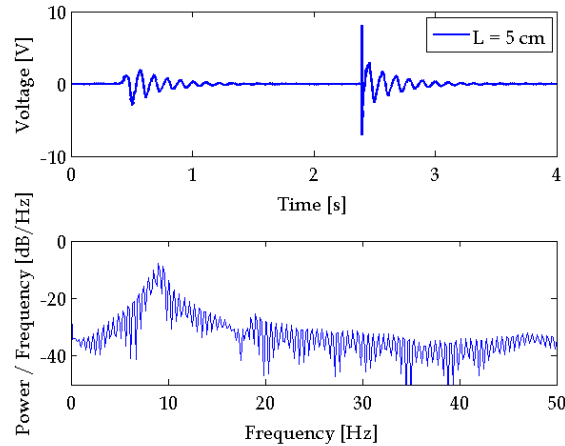


Fig. 3 A Scour Net sensor with a 5 cm exposed length was tested in air. (Top) The voltage time history responses showed the free vibration responses of the Piezo Film-PDMS sensor. (Bottom) The corresponding power spectral density function showed that the resonant frequency was 9.0 Hz

Fig. 3 shows a representative voltage time history of the Scour Net's response due to two consecutive induced free vibrations. This particular result corresponded to the case when the exposed length was 5 cm. It was clear from Fig. 3 that the sensor generated large voltages (up to 10 V) and with very high signal-to-noise ratio (i.e., as can be observed from the initial 0 V sensor response and noise floor). After performing an FFT calculation using approximately 6 s of the time-domain data, Fig. 3 also shows the corresponding frequency-domain PSD function. The resonant frequency was determined by searching for the frequency corresponding to the peak PSD. Other test results also produced similar types of data. It should be mentioned that damping was not considered in these tests, and the accuracy of the results could be affected by this fundamental assumption.

After conducting multiple sets of tests that varied the exposed length from 1 to 9 cm, one set of results was plotted as shown in Fig. 4 (i.e., averaging was not performed). First, Fig. 4 shows that the resonant frequency varied with exposed length non-linearly, which was expected. In addition, when sensor exposed lengths are short (i.e., from 1 to 5 cm), great sensitivity was observed; the resonant frequency decreased from ~ 70 Hz for the 1 cm case to ~ 10 Hz for the 5 cm case. It can be seen that frequency sensitivity decreased as length continued to increase.

Using the resonant frequencies and Eq. (5), a linear-least squares minimization method was used for determining the Young's modulus of the sensor that would best fit the theoretical exposed lengths. This minimization procedure yielded $E = 5.79$ MPa, and this value was assumed for the remainder of this study. Fig. 4 also indicates that the calculated lengths compared favorably with the theoretical values (i.e., measured using a digital caliper), and the non-linear frequency sensitivity did not adversely affect exposed length estimates. However, sources of experimental error included the assumption of an undamped SDOF model, measurement noise, and frequency resolution. Nevertheless, the results obtained were promising, since scour depth could be resolved using only one voltage output, as opposed to many discrete piezoelectric transducers per instrumented sensor location, as was proposed by Wang *et al.* (2012).

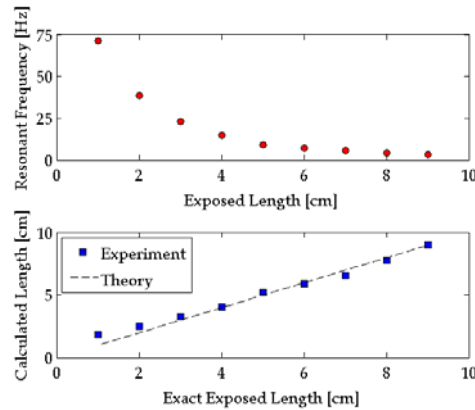


Fig. 4 (Top) The resonant frequencies for the nine different exposed lengths were extracted from the power spectral density plots. Resonant frequencies decreased with increasing scour depths. (Bottom) The calculated scour depths were also compared to theoretical results (i.e., direct measurements)

3.2 Scour depth monitoring proof-of-concept

After demonstrating that Scour Net was able to monitor sensor lengths in ambient air, the objective of this next test was to verify its operations in a wet environment. First, a 200 mL graduated cylinder was placed in the middle of a water tank (50 cm long, 25 cm wide, and 30 cm deep) to serve as a model bridge pier (i.e., for reference). Second, a 30 cm-long Scour Net prototype (i.e., encased in PDMS and attached to a PVC plate) was placed ~10 cm away from the pier, with weights placed at its footing to secure it in place. Then, the tank was filled with sand, and water was added so that the water level was ~18 cm high. A picture of the experimental setup is shown in Fig. 5. It should be noted that the Scour Net sensor protruded above the water surface. Although unrealistic in a real-world setting, this setup facilitated testing and the introduction of an initial displacement to induce free vibration of the sensor. Sensor exposed lengths were measured from the top of the Scour Net to the soil surface near the vicinity of the sensor. The generated voltage response was collected using the Agilent DAQ.

Using the aforementioned experimental setup, the exposed length of the sensor was increased from 8.5 to 17.5 cm (in 0.5 cm increments). For each length, the free vibration response of the sensor was recorded. Fig. 6 summarizes the results from the wet tests. Similar to Fig. 4, the Scour Net's resonant frequency also decreased with exposed lengths. Note that the resonant frequencies plotted in Fig. 6 were different than the results from the dry tests discussed in Section 3.1 (Fig. 4); this was because the Scour Net employed here was attached to a stiffer PVC bar. Nevertheless, the results confirmed the operation of the design in a wet environment. The Scour Net was waterproofed by the PDMS coating, and the sensor's response remained stable throughout the various tests. While PDMS served its purpose for waterproofing, its properties in complex real-world conditions still need to be studied. It is likely that future designs will employ robust marine epoxies instead, combined with a more durable outer casing and with smaller profiles, to prevent localized scouring at instrumented locations.



Fig. 5 A picture of the Scour Net being tested in a wet environment is shown. The experiment entailed placing a sensor in close proximity of the model graduated cylinder bridge pier

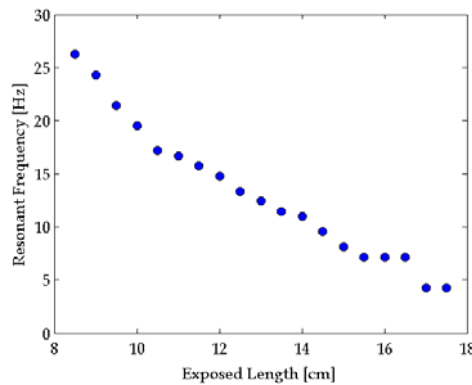


Fig. 6 The Scour Net in the water tank was subjected to free vibration testing. Exposed length was varied from 8.5 to 17.5 cm (in 0.5 cm increments). As expected, the system's resonant frequency decreased as scour depth increased

4. Distributed scour monitoring

The goal of the last test was to demonstrate the feasibility of a densely distributed Scour Net system for monitoring scour hole topography and evolution. Here, 11 sensors were fabricated and mounted on top of a Newport optics table similar to Fig. 2. Scour Net sensors were separated 20 cm apart from one another, and the layout of the sensors is schematically illustrated in Fig. 7. The location where the bridge pier was at (i.e., modeled using a graduated cylinder) did not have a Scour Net sensor installed.

A total of three sets of scour topography monitoring tests were conducted in ambient air. For each of the three test cases, a hypothetical scour hole shape was defined, and the scour depths at the different sensor locations (Fig. 7) are listed in Table 1 (see columns labeled 'Theory'). Scour depth at each sensor location was set by manually adjusting the mount. A digital caliper was also used for confirming sensor exposed lengths. The next step was to collect data from the cantilevered Scour Net sensors. Since the Agilent MSO8104A only had four channels, at most four sensors could be simultaneously interrogated for measuring their voltages during free vibrations.

The DAQ was then disconnected and then reconnected to another set of sensors, and free vibration tests were conducted again. After several sets of data were obtained from each of the 11 Scour Net sensors, the mounts were adjusted to reflect the next scour hole topography as shown in Table 1, and the same testing procedures were repeated. Future tests will utilize a multi-channeled DAQ and more reasonable sampling rates (e.g., 200 to 1,000). The influence of sampling rate and DAQ noise will also be investigated to see how they affect the resolution and accuracy of calculated scour depths.

Table 1 Summary of scour topography monitoring results*

Sensor #	Scour hole #1		Scour hole #2		Scour hole #3	
	Theory	Experiment	Theory	Experiment	Theory	Experiment
1	2	2.95	3	3.43	4	4.22
2	2	2.88	3	3.73	5	5.47
3	2	2.97	3	3.59	5	5.20
4	2	2.93	3	3.90	4	4.89
5	2	3.06	4	3.70	6	4.65
6	2	2.95	4	4.44	6	6.07
7	2	2.67	3	4.00	5	5.40
8	2	3.15	3	3.92	4	5.57
9	2	3.18	3	3.97	5	5.08
10	2	2.84	3	3.34	5	5.12
11	2	3.09	3	3.88	4	5.21

* All results are presented in units of centimeters, and sensor # corresponds to those shown in Fig. 7.

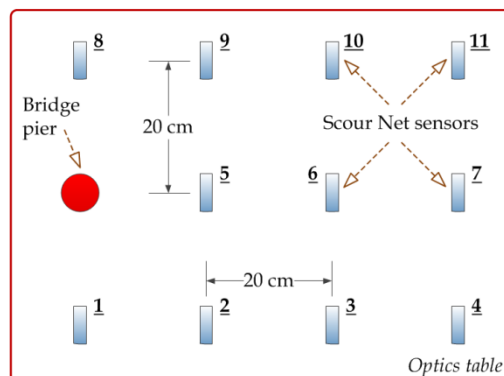


Fig. 7 The layout of the 11 distributed Scour Net sensors mounted on top of an optics table is shown. Sensor IDs are labeled in bold and underlined

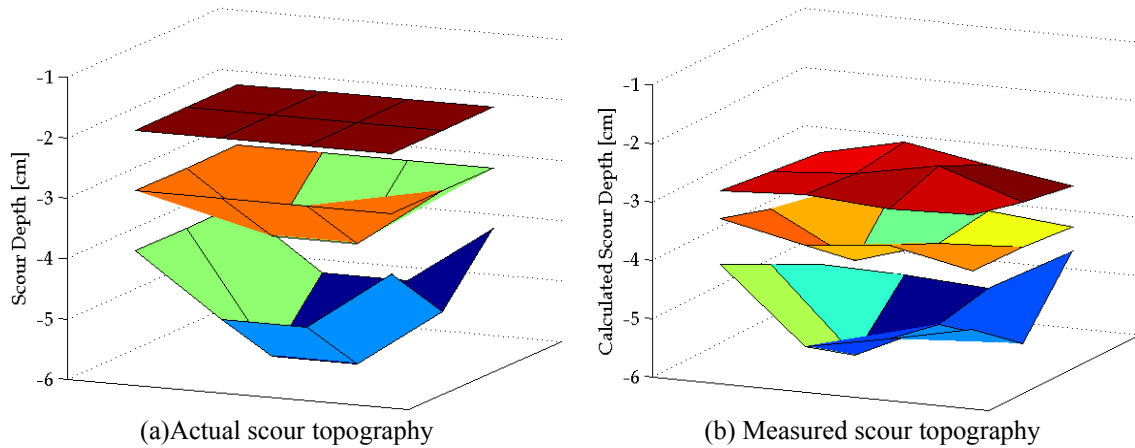


Fig. 8 The 11 distributed Scour Net sensors were interrogated during free vibration, and their results were processed to back-calculate scour depths. The (a) actual and (b) experimental results are presented

Table 1 summarizes the results for one set of tests corresponding to each of the three simulated scour holes. These results were also plotted in 3D as shown in Fig. 8. It should be noted that, to generate these surface plots in *MATLAB*, data at the bridge pier (where there was no sensor) was needed. Thus, it was assumed that the scour depth at the pier was the average of the depths measured by sensors #1 and #8 (refer to Fig. 7). These results shown in Fig. 8 confirmed that a densely distributed Scour Net sensing network would be able to provide measurements of scour hole shape, size, and their evolution with time (i.e., at least in a controlled, dry, laboratory environment). Although this study utilized static testing, the results successfully proved the monitoring concept, strategy, and methodology. From Table 1 and Fig. 8, it is obvious that discrepancies were observed. Closer inspection of each Scour Net sensor found that the Piezo Films and the PDMS substrates were not cut to be perfectly rectangular, and subtle geometrical changes could have introduced significant errors. The calculations also relied on an estimated Young's modulus, which was obtained from one set of data from a single sensor specimen. Continued work will focus on a more robust manufacturing method so as to minimize fabrication inconsistencies, as well as more rigorous and realistic experimental testing and models.

5. Conclusions

This study presented a novel piezoelectric Scour Net sensing system for monitoring scour hole topography and its evolution in time. First, the Scour Net sensor was based on depositing or embedding a continuous piezoelectric film in an elastomer substrate. Time-domain sensor voltage measurements were mapped to the frequency-domain for calculating sensor exposed lengths (or scour depths). The instrumentation of multiple sensors formed the distributed scour topography monitoring system.

Three different sets of experiments were conducted. First, a prototype Scour Net was mounted and set up as a cantilevered structure. Its length was varied, and the sensor's generated voltage response due to free vibration in ambient air was measured. The data was processed in *MATLAB*,

which calculated the exposed length of the sensor by assuming that it was an SDOF system. The results matched closely with digital caliper measurements of the actual specimen after calibration. Then, a waterproofed version of the sensor was also tested in a water tank with soil, water, and a model bridge pier. The depth of the soil was varied, and free vibration response of the sensor was again recorded. As expected, sensor resonant frequencies (which was related to scour depth) decreased as the scour depth increased. Lastly, 11 nearly identical sensors were fabricated and were all mounted on an optics table (in a dry state) to simulate a distributed scour topography monitoring system. The sensors were subjected to three unique simulated scour hole topographies, and the 3D scour hole could be determined based on sensor measurements. Although some discrepancies were observed, future work would focus on improving manufacturing, considering damping, and measuring the Young's modulus of the sensing strip to improve estimation accuracy and resolution. Testing and operations in realistic wet or riverine environments (with turbulent flow) will also be considered.

Acknowledgements

The authors gratefully acknowledge the National Science Foundation (NSF) for the support of this research (grant number CMMI-1234080 and Hazard Mitigation and Structural Engineering (HMSE) program manager: Dr. Kishor Mehta). Ms. Faezeh Azhari is also acknowledged for her assistance with experimental preparation and data processing. Partial support was also provided by the College of Engineering, University of California, Davis.

References

- Ayres. (2004), Field manual - scour critical bridges: High-flow monitoring and emergency procedures. Boise, Idaho: Idaho Department of Transportation.
- Barkdoll, B.D., Ettema, R. and Melville, B.W. (2007), NCHRP report 587 - countermeasures to protect bridge abutments from scour. Washington DC: Transportation Research Board, 1-216.
- Deng, L. and Cai, C.S. (2010), "Bridge scour: Prediction, modeling, monitoring, and countermeasures - a review", *Pract. Period. Struct. Des. Constr.*, **15**(2), 125-134.
- Gee, K.W. (2008), Action: National bridge inspection standards - plan of action for scour critical bridges. *Federal Highway Administration (FHWA)*. Washington DC.
- Hunt, B.E. (2009), NCHRP synthesis 396 - monitoring scour critical bridges. Washington DC: Transportation Research Board, 1-65.
- Lin, Y.B., Lai, J.S., Chang, K.C. and Li, L.S. (2006), "Flood scour monitoring system using fiber bragg grating sensors", *Smart Mater. Struct.*, **15**(6), 1950-1959.
- Liu, Y.T., Tong, J.H., Lin, Y., Lee, T.H. and Chang, C.F. (2010), "Real-time bridge scouring safety monitoring system using mobile wireless technology", *Proceedings of the IEEE 4th International Conference on Genetic and Evolutionary Computing*.
- Lueker, M., Marr, J., Ellis, C., Hendrickson, A. and Winsted, V. (2010), "Bridge scour monitoring technologies: Development of evaluation and selection protocols for application on river bridges in Minnesota", *Proceedings of the International Conference on Scour and Erosion 2010*, 949-957.
- Radchenko, A., Pommerenke, D., Chen, G., Maheshwari, P., Shinde, S., Pilla, V. and Zheng, Y.R. (2013), "Real time bridge scour monitoring with magneto-inductive field coupling", *Proceedings of SPIE - Smart Structures/NDE*. San Diego, CA, 86922A.
- Ryu, D., Loh, K.J., Ireland, R., Karimzada, M., Yaghmaie, F. and Gusman, A.M. (2011), "In-situ reduction

- of gold nanoparticles in PDMS matrices and applications for large strain sensing”, *Smart Struct. Syst.* **8**(5), 471-486.
- Schall, J.D. and Davies, P. (1999), “Instrumentation for measuring scour at bridge piers and abutments”, *TR News*, 32-33.
- Schall, J.D., Price, G.R., Fisher, G.A., Lagasse, P.F. and Richardson, E.V. (1997), NCHRP report 397a - sonar scour monitor: Installation, operation, and fabrication manual. Washington DC: Transportation Resesarch Board, 1-38.
- Schneider, F., Fellner, T., Wilde, J. and Wallrabe, U. (2008), “Mechanical properties of silicones for MEMS”, *J. Micromech. Microeng.*, **18**(6), 065008.
- Wang, C.Y., Wang, H.L. and Ho, C.C. (2012) “A piezoelectric film type scour monitoring system for bridge pier”, *Adv. Struct. Eng.*, **15**(6), 897-906.
- Wang, T.T., Herbert, J.M. and Glass, A.M. (1988), *The applications of ferroelectric polymers*, London: Blackie and Son Ltd.
- Zarafshan, A., Iranmanesh, A. and Ansari, F. (2012), “Vibration-based method and sensor for monitoring of bridge scour”, *J. Bridge Eng.*, **17**, 829-838.
- Zhou, Z., Huang, M., Huang, L., Ou, J. and Chen, G. (2011), “An optical fiber bragg grating sensing system for scour monitoring”, *Adv. Struct. Eng.*, **14**(1), 67-78.